

Preliminary Studies of the Disposition of Cesium in a Glass-Bonded Sodalite Waste Form

Marsha J. Lambregts and Steven M. Frank
Argonne National Laboratory-West, PO Box 2528, Idaho Falls, ID 83401

ABSTRACT

Argonne National Laboratory has developed an electrometallurgical treatment for DOE spent metallic nuclear fuel. Fission products are immobilized in a durable glass bonded sodalite ceramic waste form (CWF) suitable for long term storage in a geological repository. Cesium is estimated to be in the waste form at approximately 0.1 wt.%. The exact disposition of cesium was uncertain and it was believed to be uniformly distributed throughout the waste form. A correlation of X-ray diffractometry (XRD), electron microscopy (EM), and nuclear magnetic resonance spectroscopy (NMR) performed on surrogate ceramic waste forms with high cesium loadings found a high cesium content in the glass phase and in several non-sodalite aluminosilicate phases. Cesium was not detected in the sodalite phase.

INTRODUCTION

Argonne National Laboratory has recently completed the Spent Fuel Demonstration Project for the DOE involving the use of electrometallurgical conditioning of spent metallic nuclear fuel. This process uses a molten lithium chloride/potassium chloride eutectic salt to anodically dissolve the fuel. Three materials are produced during this process [1]: uranium, cladding hulls and the fission product bearing salt. Various isotopes of cesium reside in the salt. From a repository point of view, cesium-135 is particularly problematic because of its high radioactivity and high solubility in water.

The CWF developed to immobilize the salt is composed primarily of two phases—sodalite and glass [2]. Minor phases present in the CWF include: nepheline, halite crystallites, rare earth silicates and actinide oxides. The sodalite is produced from a solid state reaction of salt with zeolite 4A under heat or heat and pressure. Production of the CWF involves heated mixing of dry zeolite A powder with ground, sieved salt from the electrorefiner at 500°C. A glass binder is mixed in at a 1 to 3 ratio with the salt-occluded zeolite. The mixture is heated to 915°C. It is during this step that the zeolite transforms into sodalite and the glass melts, binding the sodalite particles together into a consolidated waste form.

Sodalite contains chlorine as part of the crystal structure. The empirical formula for sodalite is $M_8Al_6Si_6O_{24}X_2$, where M is a metal and X represents halides. The overall structure is cubic and consists of alternating SiO_4 and AlO_4 tetrahedra joined at the corners to form four unit and six unit rings. These rings make up beta-cages similar to those found in zeolite 4A. For the sodium chloride form of sodalite, a chlorine atom lies in the center of each cage tetrahedrally coordinated to four sodium atoms. The sodium atoms are further coordinated to the oxygen atoms of the six unit rings.

The cesium content of the CWF is approximately 0.1% by weight. The fission product cesium was detected in the waste form via gamma spectroscopy but analysis by X-ray diffractometry and electron microscopy were unable to detect any cesium bearing phases. To investigate how cesium is incorporated into the waste form, surrogate CWF samples were produced with higher concentrations of cesium.

The purpose of this investigation was to determine the disposition of cesium in the CWF. XRD, EM and NMR were employed to achieve this goal on both a macroscopic and microscopic level.

EXPERIMENTAL

Two samples of surrogate CWF were produced containing 100% cesium chloride (CsCl) and 1:1 CsCl:NaCl. (Sodium chloride was chosen initially instead of eutectic salt as a diluent to simplify the system.) A similar method to the actual process, but on a smaller scale, was used for the production of these samples. For the 1:1 blend, the salts were weighed, mixed and melted. The resulting salt was cooled and remelted to ensure complete mixing. Then the salt was ground and screened to approximately the same dimensions as the zeolite powder. In both cases the appropriate amounts of salt and zeolite were transferred to a small v-mixer and heated to 550°C while mixing to achieve salt occlusion. Salt occlusion was monitored by mixing 0.5g of salt-occluded zeolite with 30g of distilled deionized water for 1 minute and immediately filtering the solution. The chloride level in the filtrate was measured using an ion specific electrode. Samples were mixed with borosilicate glass frit at a 3:1 salt-occluded zeolite to glass ratio by weight. Approximately 35 grams of the mixture was transferred to graphite crucibles and heated to 915°C for four hours and cooled. All processes were performed in an argon atmosphere. The resulting waste forms, while not as compacted as the true wastefrom, were well formed.

Samples of the high cesium CWF's were finely ground for XRD and NMR analysis. Pieces of the samples were mounted in epoxy and polished for the EM analysis. XRD and EM were performed using a Scintag X1 (Cu K α) and a Zeiss DSM 960 respectively. Several nuclear magnetic resonance active nuclei are present in the surrogate CWF samples such as ²⁹Si, ²⁷Al, ³⁵Cl, ²³Na and ¹³³Cs. Both a Bruker 11.7T and 7.04T Avance NMR spectrometers were used to study these nuclei.

RESULTS

X-ray diffractometry

Figure 1 shows XRD scans of the samples. Sodalite and a form of pollucite (CsAlSi₂O₆) can be positively identified in the scans. Other unidentified, minor phases are also present. In addition the broad rise in the background intensity near 25° 2 θ is consistent with the presence of a glass phase. The patterns are identical with respect to the sodalite phase, but the pollucite phase is decreased in intensity in the 1:1 Cs:Na CWF as are the other minor unidentified phases.

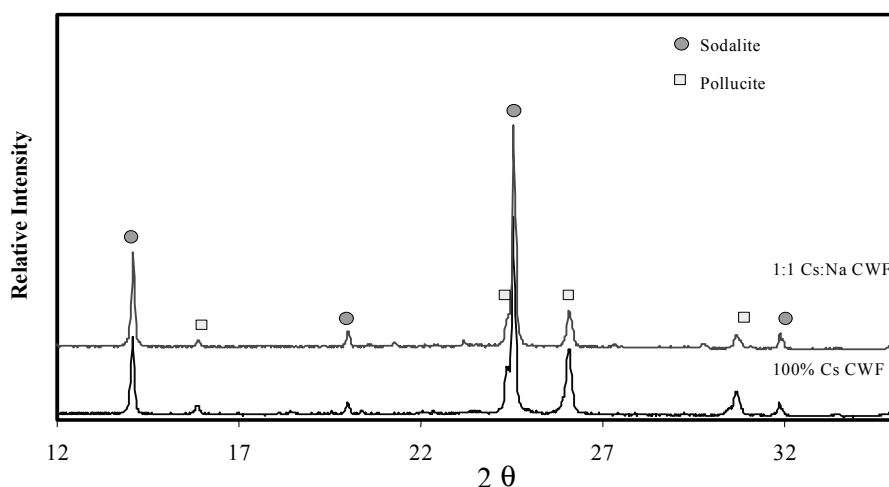


Figure 1. XRD patterns for 100% Cs CWF and 1:1 Cs:Na CWF.

Nuclear magnetic resonance spectroscopy

Figures 2,3 and 4 show the NMR spectra acquired on the two samples. In figure two, the ^{29}Si spectra show a broad peak at approximately -100 ppm and two sharper peaks at -88 ppm and -84.5 ppm and a shoulder at -83.7 ppm. The ^{27}Al NMR spectra show a large peak at 64 ppm with a pronounced shoulder at approximately 59.5 ppm, some broadening at the base. In figure 3, the ^{23}Na NMR spectra show one sharp peak and two broad resonances. The ^{35}Cl NMR shows one very sharp peak. The ^{133}Cs NMR spectra in figure 4 show a broad resonance at approximately 0 ppm. The most interesting features, however, are the three peaks at -30 , -42 and -56.4 ppm.

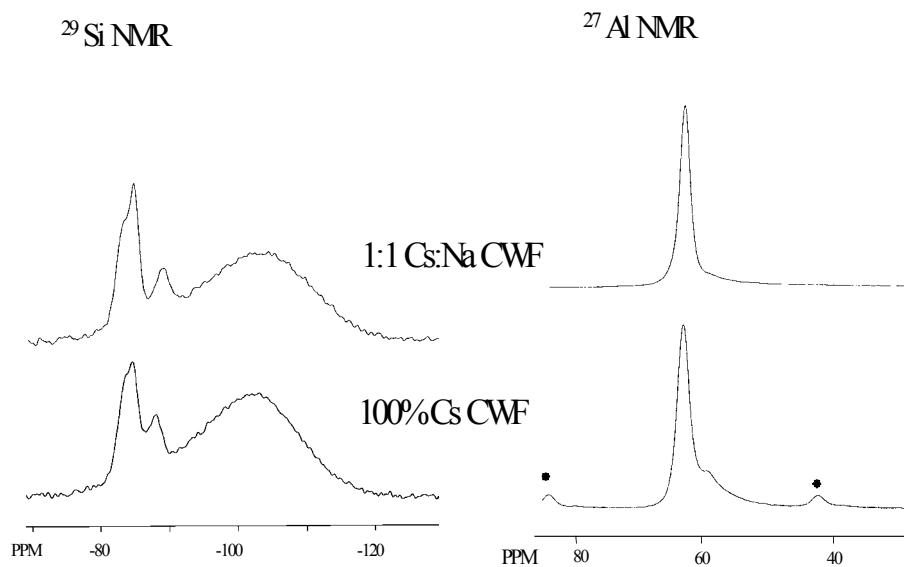


Figure 2. ^{29}Si and ^{27}Al Magic Angle Spinning (MAS) NMR spectra of 100% Cs CWF and 1:1 Cs:Na CWF. Spectra were acquired on a 7.04T Bruker NMR spectrometer. 100% Cs CWF ^{29}Si NMR spectra were acquired with 2048 scans. The 1:1 Cs:Na CWF ^{29}Si NMR spectra were acquired with 1112 scans using a pulse delay of 150 seconds. The ^{27}Al NMR spectra were acquired 16 scans using a 5 second pulse delay. Spinning speed for ^{29}Si NMR and 1:1 Cs:Na

CWF ^{27}Al spectra was 6000 Hz. The 100%Cs CWF ^{27}Al NMR spectrum spinning speed was 2000 Hz.

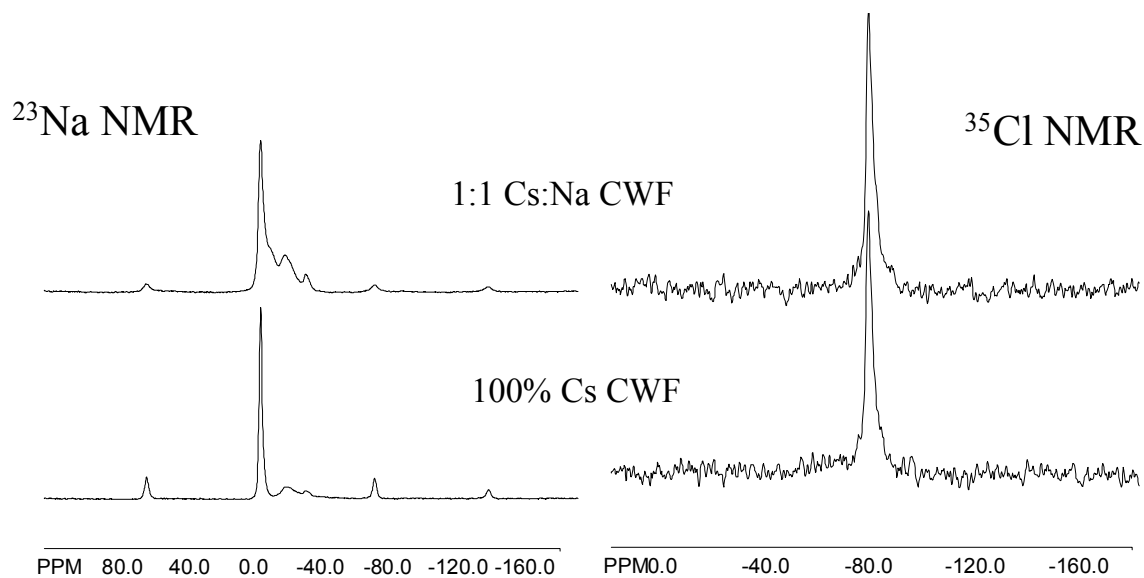


Figure 3. ^{23}Na and ^{35}Cl MAS NMR spectra of 100% Cs:Na CWF and 1:1 Cs:Na CWF. Spectra were acquired on a 11.7 T Bruker NMR spectrometer. Spin rate for the ^{23}Na NMR spectra was 9000Hz for 132 scans using a pulse delay of 1 second. Spin rate for the ^{35}Cl spectra was 6800 Hz for 664 scans using a pulse delay of 1 second.

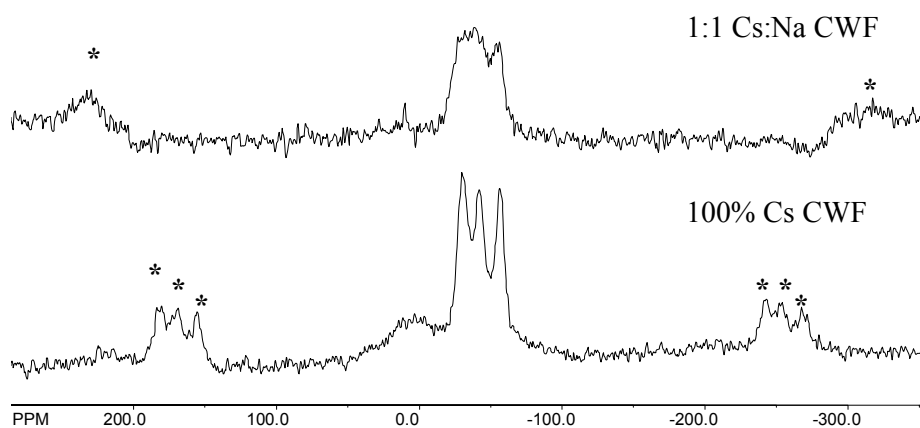


Figure 4. ^{133}Cs MAS NMR spectra of 100% Cs CWF and 1:1 Cs:Na CWF. Spectra were acquired on a 11.7 T Bruker NMR spectrometer. Spin rate was 14.2 kHz for 1338 scans and a pulse delay of 0.5 seconds for the 100% Cs CWF. Spin rate was 16.9 kHz for 5071 scans and a pulse delay of 0.5 seconds for the 1:1 Cs:Na CWF.

Electron Microscopy

Figure 5 shows backscatter electron (BSE) micrographes of both waste forms. The multiphase nature of the waste form is evident. White areas are indicative of the high cesium areas, even light gray areas indicate the glass regions and the more mottled darker gray areas are the sodalite. The black regions are the epoxy mount material. Five different regions were identified and elemental analyses were performed on these. These regions are high cesium content areas, sodalite, glass, a boundary region between the glass and sodalite which is high in cesium, and spots within the sodalite which contain high cesium levels. Figure 6 shows the x-ray maps for the 100% CsCl CWF.

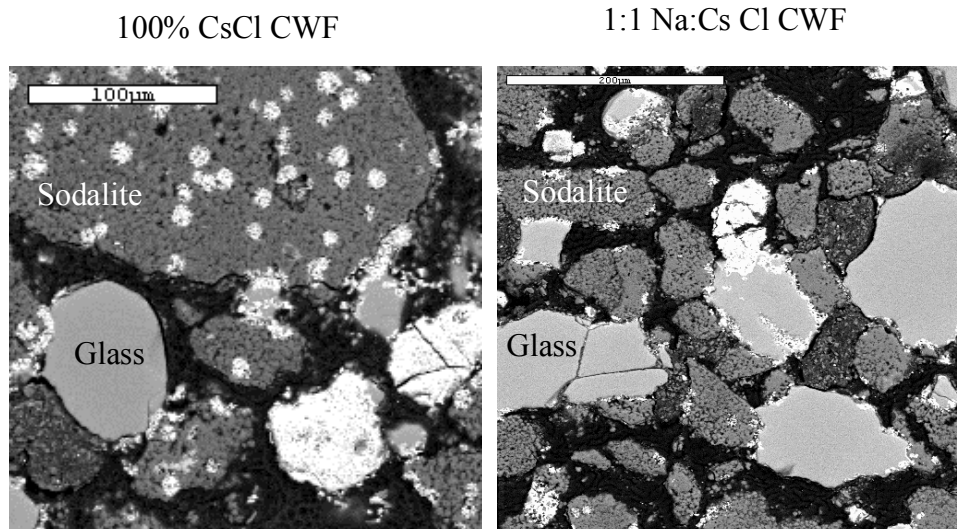


Figure 5. BSE EM micrographes of the 100% CsCl CWF and the 1:1 Na:Cs Cl CWF.

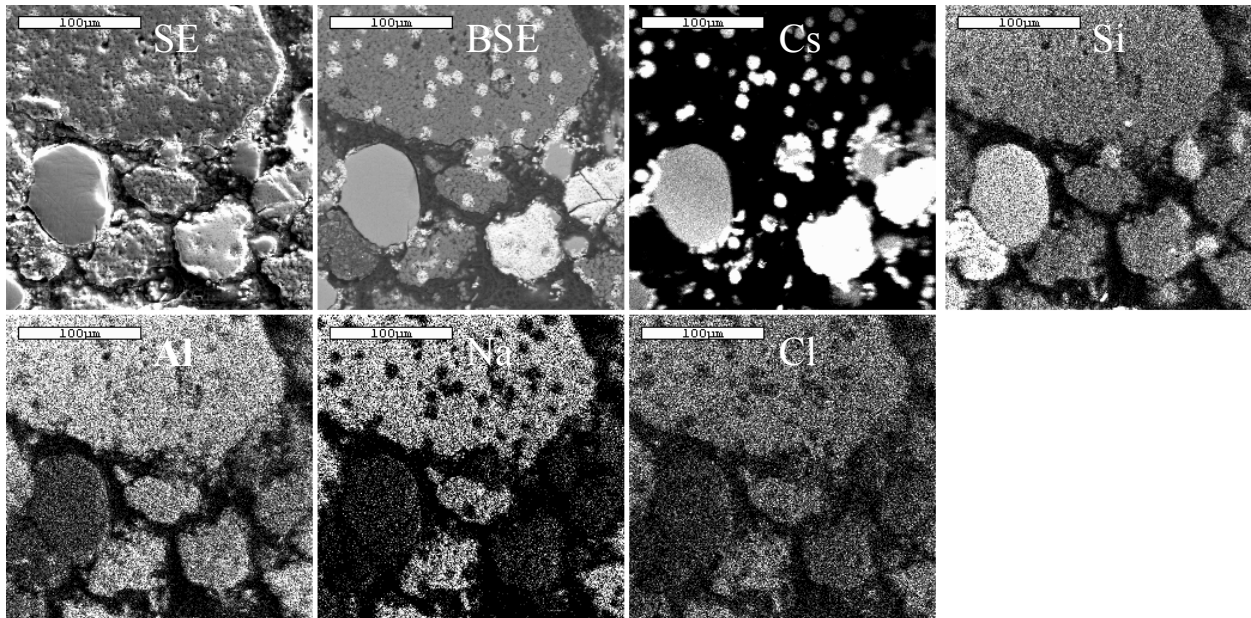


Figure 6. Secondary Electron (SE), BSE, Cs, Si, Al, Na and Cl x-ray maps of the 100% Cs CWF. Areas lighter in contrast correspond to greater concentration of each element.

These maps emphasize the differences in concentration of the various elements within the waste form. These micrographes show the concentration of the cesium in the lighter spots within the sodalite and on the surface of some particles and the lack of chlorine in these same areas. Figure 7 shows a line scan across a sodalite particle—through a high cesium spot, the sodalite phase, the boundary phase and on into the center of a glass phase region. Note the concentration changes particularly in the cesium and chlorine scans.

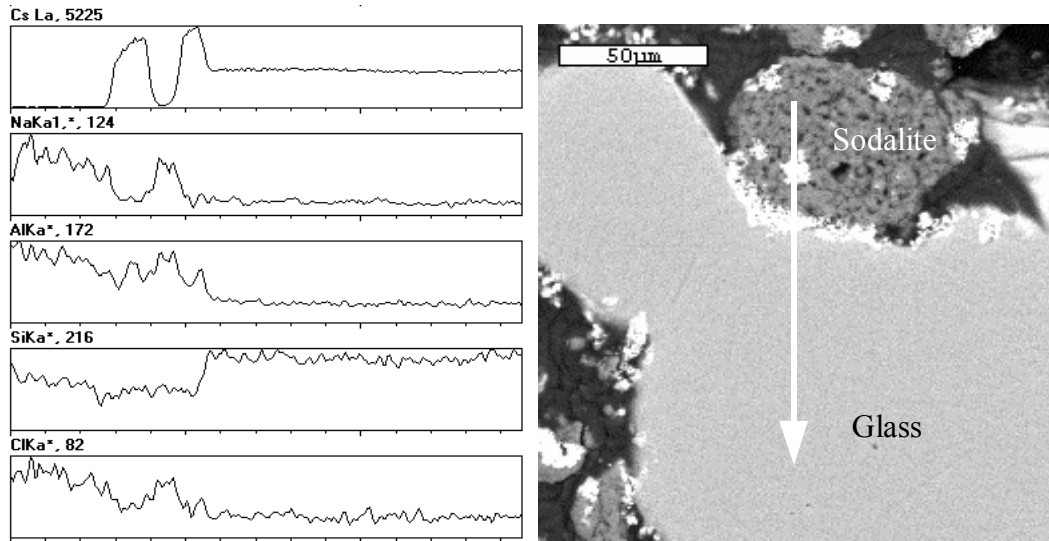


Figure 7. This figure denotes a x-ray analysis line scan across a section of the 100% Cs CWF.

X-ray analysis indicates that the high cesium level pieces and the high cesium spots within the zeolite have similar Si:Al:O ratios and may be the same phase, see Table 1 for ratios. The boundary region has a highly variable composition.

Table 1. SEM x-ray spectroscopic analysis elemental ratio's and weigh percentages for 100% Cs CWF.

Element	Sodalite		Glass		Spots in sodalite		High Cs pieces		Boundary region	
	Atom %	Wt. %	Atom %	Wt. %	Atom %	Wt. %	Atom %	Wt. %	Atom %	Wt. %
Na	10.5	11.6	1	0.89	1	0.83	3	2.48	1	1.14
Cs	0	0	3	17.1	7	33.5	7	33.5	5	33.2
Al	14.8	19.5	3	3.54	12.5	12.1	12.5	12.1	7	9.44
Si	14.5	19.8	24	30	16	16.7	15.8	16.5	14	20.3
O	55.3	41	69	48.2	64	36.8	61.6	35.4	45	36
Cl	4.9	8.2	0	0	0	0	0	0	0	0

DISCUSSION

The EM data gives the best initial description of the high cesium CWF showing the glass, sodalite and high cesium content aluminosilicate phases. This ties in well with the XRD indication of the major sodalite and pollucite phases. The sodalite phase matches well to library patterns of sodium sodalite [3]. The substitution of other cations such as lithium and potassium

for sodium in the sodalite phase leads to a shifting of the XRD pattern to either higher or lower 2Θ values. If cesium were in the sodalite lattice it would also be expected to shift the XRD pattern. This is not found in the XRD patterns of these high cesium CWF samples. Cesium was also not detected in the sodalite phase via wavelength dispersion spectroscopy on the EM.

The ^{35}Cl NMR data suggests that the chlorine atoms are in a single, highly symmetric environment. This is indicated by the sole sharp resonance found in the spectrum. Chlorine is a quadrupolar nuclei with a large quadrupolar coupling constant and as such would be expected to have complex broad resonances if not in a symmetric environment. This agrees with the known structure of sodium chloride sodalite having a highly symmetric environment where the chlorine atom is tetrahedrally coordinated to four sodium atoms. The EM analysis confirms this by indicating that the chlorine is only found in the pure sodalite regions in the waste form. No halide salts were detected in the NMR spectra or XRD patterns.

Of the NMR active nuclei in this study only ^{29}Si has a nuclear spin of $1/2$. It has very well characterized though somewhat overlapping spectral regions that correlate to the number of Si-O-Al bonds [4]. Silicon atoms exhibiting resonances in the region -82 to -92 ppm are bound through oxygen to four aluminum atoms. Silicon atoms exhibiting resonances in the region of -85 to -95 ppm are bound through oxygen to three aluminum atoms and a single silicon atom. Silicon atoms exhibiting resonances in the region of -92 to -100 ppm are bound through oxygen to two aluminum atoms and two silicon atoms, -98 to -108 ppm through oxygen to a single aluminum and three silicon atoms and -102 to -117 ppm through oxygens to four other silicon atoms. The assignments of the peak at -84.5 ppm to sodalite, the broad peak at ~ 100 ppm to glass, the peak at -88 ppm to pollucite are consistent with literature and example compounds. The shoulder at -83.7 ppm is most likely due to silicon bonded through oxygen to four other aluminum atoms and comes from the other cesium aluminosilicate phases present in the sample.

In the ^{27}Al NMR spectra all of these peaks fall in the range of tetrahedrally coordinated aluminum. Octahedral aluminum resonances fall close to zero ppm. This correlates well with the sodalite and pollucite phases seen in the XRD scan. The large peak is due to the sodalite and the shoulder is most likely the pollucite phase. The underlying broadening of the central peak could be a similar aluminum environment to that of sodalite and may relate to one of the chemically variable, unidentified phases. Though ^{27}Al is also a quadrupolar nuclei and can exhibit peak splitting and broadening due to its nuclear spin of $5/2$, it is in a relatively symmetric environment in its tetrahedral coordination in sodalite.

Interpretation of the ^{23}Na NMR is difficult due to the quadrupolar nature of the nuclei. The sharp peak is due to the sodalite, one of the broad resonances is due to glass and the other is due to another sodium bearing unidentified species.

In the ^{133}Cs NMR, there is a small broad resonance at about 0 ppm, which is assigned to pollucite based upon comparison to synthetic pollucite produced in our laboratory and identified via XRD. Literature values for the cesium chemical shift for pollucite were given by Teerstra et al.[5] Which show the chemical shift versus 1 M CsCl at -49 ppm for both a natural and synthetic pollucite. The samples in this study do not agree with this value. It is possible, that given the variable composition of what is identified as the pollucite phase: the boundary high cesium region, that the environment of the cesium is sufficiently different to warrant the change in chemical shift. The chemical shifts for the three sharp peaks in the spectrum are within the range for cesium resonances found for cesium in other aluminosilicate systems.[6,7,8]It is possible that these shifts are due to the as yet unidentified high cesium aluminosilicate phases indicated by the EM data. It is obvious from the EM data that the glass has a preference for the

cesium as its composition is 17%Cs in the 100% cesium waste form and 14% in the 50% cesium waste form. Originally the glass contains no cesium. A 30% cesium glass was made in our laboratory and analyzed by NMR. This spectrum showed only a very low intensity, extremely broad band stretching across over 500 ppm. This agrees with the literature spectra for cesium containing glass systems[9]. The low intensity of the glass phase cesium resonance coupled with the fact that only 25% of the waste form is glass prevents its detection in the NMR spectra.

CONCLUSIONS

For high cesium surrogate CWF materials, cesium is detected in the glass and in several non-sodalite aluminosilicate phases. Cesium is not detected in the sodalite phase. The implications for the actual ceramic waste form are that the cesium is preferentially found in the glass. It also is not part of the sodalite but could form alternative discrete cesium aluminosilicate phases.

ACKNOWLEDGEMENTS

This work was supported by the U.S. Department of Energy, Nuclear Energy Research and Development Program, under Contract No. W-31-109-ENG-38. Special thanks to Tanya M. Barber and Tom O'Holleran for operational assistance with the EM and to Dr. Thomas Luther and Dr. Alexander Blumenfeld for their operational assistance with the NMR spectrometers and Dr. Chien M. Wai for his support of this work as part of a doctoral project.

REFERENCES

1. K.M. Goff, S.G. Johnson, M.F. Simpson, R.W. Benedict, R.D. Mariani, B.R. Westphal in Proceedings of the Embedded Topical Meeting on DOE Spent Nuclear Fuel and Fissile Material Management (Amer. Nucl. Soc. Proc. San Diego, Ca., 2000) pp. 58–63.
2. T.L. Moschetti, W. Sinkler, T. DiSanto, M.H. Noy, A.R. Warren, D. Cummings, S.G. Johnson, K.M. Goff, K.J. Bateman, and S.M. Frank in Scientific Basis for Waste Management XXIII, edited by R.W. Smith, D.W. Shoosmith, (Mater. Res. Soc. Proc. 608, Boston, Ma., 2000) pp. 577-582.
3. International Centre for Diffraction Data, Powder Diffraction File, card number 37-0476, Newtown Square, PA(1995).
4. H.S. Jacobsen, P. Norby, H. Bildsoe, and H.J. Jakobsen *Zeolites*, **9**, 491(1989).
5. D. K. Teerstra, B. L. Sherriff, Z. Xu and P. Cerny *Can. Mineralogist*, **32**, 69(1994).
6. M.K. Ahn and L. E. Iton *J. Phys. Chem.* **93**, 4924(1989).
7. T. Tokuhiro, M. Mattingly, L.E. Iton, and M.K. Ahn *J. Phys. Chem.* **93**, 5584(1989).
8. M. K. Ahn and L. E. Iton *J. Phys. Chem.* **95**, 4496(1991).
9. R.. Dupree, D. Holland and D.S. Williams *J. Non. Cryst. Solids* **81**, 185(1986).